Rotating Wigner molecules and spin-related behaviors in quantum rings

2008 J. Phys.: Condens. Matter 20 295202

(http://iopscience.iop.org/0953-8984/20/29/295202)

J. Phys.: Condens. Matter **20** (2008) 295202 (11pp) doi:10.1088/0953-8984/20/29/295202

Rotating Wigner molecules and spin-related behaviors in quantum rings

Ning Yang, Jia-Lin Zhu[1] and Zhensheng Dai

Department of Physics and Center for Quantum Information, Tsinghua University, Beijing 100084, People's Republic of China

E-mail: zjl-dmp@tsinghua.edu.cn

Received 30 November 2007, in final form 24 April 2008
Published 26 June 2008
Online at stacks.iop.org/JPhysCM/20/295202

Abstract

The trial wavefunctions for few-electron quantum rings are presented to describe the spin-dependent rotating Wigner molecule states. The wavefunctions are constructed from the single-particle orbits which contain two variational parameters to describe the shape and size dependence of electron localization in the ring-like confinement. They can explicitly show the size dependence of single-particle orbital occupation to give an understanding of the spin rules of ground states without magnetic fields. They can also correctly describe the spin and angular momentum transitions in magnetic fields. By examining the von Neumann entropy, it is demonstrated that the wavefunctions can illustrate the entanglement between electrons in quantum rings, including the AB oscillations as well as the spin and size dependence of the entropy. Such trial wavefunctions will be useful in investigating spin-related quantum behaviors of a few electrons in quantum rings.

(Some figures in this article are in colour only in the electronic version)

1. Introduction

The few-electron semiconductor quantum dots [1] have attracted a great deal of attention due to their theoretical meaning to strong correlation systems and application potential in future quantum electronics, spintronics and quantum information devices. Recent studies have shown that there are liquid-to-crystal transitions of electronic states in few-electron quantum dots with the change of dot size or magnetic field. The energy spectrum [2], correlation [3] and entanglement have different characters in liquid-like and crystal-like states. In strong magnetic fields, the ground states in quantum dots become rotating Wigner molecules (RWMs) [4–6] which are electronic states with crystal correlations and without any symmetry breaking.

Benefiting from the developments of manufacturing and experimental techniques, the studies of quantum dots with the ring-like geometry, namely quantum rings [7, 8], have been an increasing topic in low-dimensional physics. Experimentally, the electrons in the ring can be precisely controlled down to quite a small number. The topology of the ring makes the system appropriate to observe the Aharonov–Bohm (AB) oscillations [9, 10] with the changes of the magnetic flux. Theoretically, in one- or quasi-one-dimensional systems, the Coulomb interaction brings strong correlations between electrons and leads to non-Fermi liquid behavior [11, 12]. For the quantum rings with a few electrons, both the energy level structures and the characters of spectroscopies reflect the correlations between particles and cannot be understood within a single-particle picture [13]. The idea of rotational and vibrational states of localized electrons [12] has been proposed to understand the energy spectrum structures of quantum rings. When the electron number is small, the exact diagonalization (ED) of the many-body Hamiltonian with exact interactions is feasible. It has also provided the evidence of forming RWMs [14, 15]. In quantum rings, the crystallization is the result of strong long-range correlation and is much more easy in both magnetic fields and the field-free condition than that in quantum dots. The investigations have also revealed that the spin of the ground state may depend on the shape and size of the ring [14, 16].

For quantum dots, there have been in-depth studies on the theory of RWMs. The few-electron rotational–vibrational states in the Eckart frame have been employed to understand the magic angular momenta and spin correlations of electron molecular states in magnetic fields [17, 18]. Yannouleas and

[1] Author to whom any correspondence should be addressed.

Landman have investigated a set of trial wavefunctions for fully polarized RWMs [4] and demonstrated their accuracy by a numerical method [19]. They also proposed the projection technique [4, 20] in their work to restore both the total spin and the angular momentum symmetries for RWMs. In our previous work [21], we have derived the trial wavefunctions for four- and five-electron RWMs in quantum dots with a spin degree of freedom based on those results. Recently, the analytic four-electron states in quantum dots with spins were also investigated by Shi *et al* within the composite fermion theory, and the composite fermion crystallization [22–24] gives an understanding of the characteristics of spin correlations in crystal states in magnetic fields. These analytic functions are helpful to the study of the particle crystallization and other strongly correlated phenomena in few-electron systems [25].

Unlike the situation for quantum dots, the research on trial wavefunctions of RWMs in quantum rings is still quite limited. In this work, we will introduce a set of wavefunctions to describe RWMs in quantum rings with spin degree of freedom. Then, we take the three-electron and four-electron cases as examples to discuss the applicability of the trial wavefunctions by the comparison with the ED method. We will demonstrate that our trial wavefunctions are suitable for describing the electronic states in quantum rings with appropriate shape and size. They can give an understanding of the spin transitions and the spin rules of the ground state with the change of the ring size, and exhibit correct angular momentum transitions of RWMs with different spins in magnetic fields. Besides these, correlation and entanglement are important issues for understanding the many-body states and quantum phase transitions, so we also discuss the entanglement characters of RWMs in quantum rings based on the trial wavefunctions.

The remainder of the paper is organized as follows. The trial wavefunctions are constructed in section 2, their size and shape dependence of accuracy, the spin rules of the ground state without magnetic fields, the angular momentum transitions in magnetic fields and the entanglement characteristics of RWMs in quantum rings are discussed in section 3 followed by a summary in section 4.

2. Construction of trial wavefunctions

In this section, we construct the trial wavefunctions for RWMs in quantum rings. In order to do so, the localized single-particle orbit wavefunctions are presented at first and expanded to a set of eigenfunctions of angular momentum so as to restore the rotational symmetry of the final few-electron states. The orbital functions contain two variational parameters which reflect the degree of localization of electrons in quantum rings with different shapes and sizes. Then the few-electron trial wavefunctions with certain total spin S and the z component S_z can be obtained from a formal Hamiltonian [21].

For a few-electron quantum ring with the parabolic confinement and the long-range interaction, we introduce the modified Gaussian functions to describe the localized single-particle orbit wavefunctions (un-normalized) subjected to a perpendicular uniform magnetic field:

$$u(z) = \exp\left(-\frac{(|z| - |Z_j|)^2}{2\lambda_0^2}\right) \times \exp\left(-\frac{|z - Z_j|^2}{2\lambda^2}\right) \times \exp\left(\frac{zZ_j^* - z^*Z_j}{4l_B^2}\right), \quad (1)$$

where $z \equiv x - \mathrm{i}y = r(\cos\theta - \mathrm{i}\sin\theta)$ is the complex coordinate of the electron, and x, y and (r, θ) are the Cartesian (polar) coordinates in real space. $Z_j \equiv X + \mathrm{i}Y$ is the complex coordinate of the center of the Gaussian which can be set to one of the equilibrium positions of electrons in a circle with radius equal to the average radius R_0 of the quantum ring. The last factor is the phase factor in symmetric gauge to preserve the gauge invariance in the magnetic fields. $l_B = \sqrt{\hbar c/eB}$ is the magnetic length. The orbits contain two independent variational parameters λ and λ_0.

With polar coordinates, the normalized orbit function $u(z)$ can be expressed as

$$u(r, \theta) = \frac{1}{\sqrt{\pi\lambda\lambda'}} \exp\left(-\frac{(r - R_0)^2}{2\lambda'^2}\right) \times \exp\left\{\frac{rR_0}{\lambda^2}\left[\cos(\theta - \theta_j) + \mathrm{i}\delta\sin(\theta - \theta_j) - 1\right]\right\}, \quad (2)$$

where we have defined $\delta = \lambda^2/2l_B^2$. We also use λ' instead of λ_0 for brevity, and $1/\lambda'^2 = 1/\lambda_0^2 + 1/\lambda^2$. θ_j is the azimuth angle of the center of the Gaussian. It can be seen that, if the distribution of the orbit in the radial direction is much smaller than the radius ($r \approx R_0$), the angle and radial parts of $u(r, \theta)$ can be decoupled, λ/R_0 and λ' mainly describe the degree of localization of the single-particle orbit function in the angle and radial directions, respectively.

In order to restore the rotational symmetry of the final trial wavefunction, we can construct a set of functions ψ_l with angular momentum l, whose radial parts are the product of $\sqrt{r}$ and displaced Gaussians, and angle parts are the eigenfunctions of a particle in a one-dimensional ring

$$\psi_l(r, \theta) = (F(2))^{-1/2}\sqrt{r}\exp\left(-\frac{(r - R_0)^2}{2\lambda'^2}\right) \times \frac{1}{\sqrt{2\pi}}\exp(\mathrm{i}l\theta), \quad (3)$$

where we have defined

$$F(k) = \int_0^\infty r^k \exp\left(-\frac{(r - R_0)^2}{\lambda'^2}\right) \mathrm{d}r. \quad (4)$$

The introduction of the term $\sqrt{r}$ is to ensure the convergence of the kinetic energy expectation values of equation (3). Then the single-particle orbits $u(r, \theta)$ in equation (2) can be expanded to ψ_l as

$$u(r, \theta) = \sum_{l=-\infty}^{\infty} c_l(\theta_j)\psi_l(r, \theta). \quad (5)$$

The coefficient c_l can be determined numerically. When the electron is localized nearby to Z_j, i.e. $r \approx R_0$, $\theta \approx \theta_j$, c_l can be approximated as

$$c_l(\theta_j) = \frac{\sqrt{\lambda}F(\frac{3}{2})}{\sqrt{\pi\lambda'}R_0(F(2))^{1/2}} \exp\left(-\frac{\lambda^2}{2R_0^2}\left(l + \frac{\phi}{\phi_0}\right)^2\right) \times \exp(-\mathrm{i}l\theta_j), \quad (6)$$

where $\phi = \pi R_0^2 B$ is the magnetic flux through the circle with radius R_0 and $\phi_0 = hc/e$ is the quantum of the magnetic flux. The assumption $r \approx R_0$ is just the demand of decoupling of the radial and angular parts of the orbits, and $\theta \approx \theta_j$, which ensures $u(r, \theta)$ is well localized in the angular direction, can be satisfied when λ/R_0 is small.

For the ring with N_1 spin-up ($\uparrow$) and N_2 spin-down ($\downarrow$) electrons ($N_1 + N_2 = N$), starting with the single-particle orbits in equation (1), we can construct $C_N^{N_1}$ many-particle bases $|Z_{j_1}^{\uparrow}, \ldots, Z_{j_{N_1}}^{\uparrow}, Z_{j_{N_1+1}}^{\downarrow}, \ldots, Z_{j_N}^{\downarrow}\rangle$ with $S_z = (N_1 - N_2)/2$. Here we use sign Z_j represents the orbits $u(z)$ centered at Z_j. For large and narrow quantum rings, such a set of many-particle bases is large enough to expand the ground state and the low-lying excited states, since the electrons are well localized. Using equation (5), the many-particle bases can also be expanded as

$$\begin{aligned} &|Z_{j_1}^{\uparrow}, \ldots, Z_{j_{N_1}}^{\uparrow}, Z_{j_{N_1+1}}^{\downarrow}, \ldots, Z_{j_N}^{\downarrow}\rangle \\ &= \sum_{l_1, l_2, \ldots, l_N = -\infty}^{\infty} c_{l_1}(\theta_{j_1}) c_{l_2}(\theta_{j_2}) \ldots c_{l_N}(\theta_{j_N}) \\ &\quad \times |l_1^{\uparrow}, \ldots, l_{N_1}^{\uparrow}, l_{N_1+1}^{\downarrow}, \ldots, l_N^{\downarrow}\rangle. \end{aligned} \tag{7}$$

where sign l represents ψ_l. With the projection operator technique [4], the component with total angular momentum L can be obtained as

$$\begin{aligned} &|Z_{j_1}^{\uparrow}, \ldots, Z_{j_{N_1}}^{\uparrow}, Z_{j_{N_1+1}}^{\downarrow}, \ldots, Z_{j_N}^{\downarrow}\rangle_L \\ &= \sum_{\substack{l_1 + l_2 + \cdots + l_N = L \\ l_1 < l_2 < \cdots < l_{N_1} \\ l_{N_1+1} < \cdots < l_N}}^{l_1 + l_2 + \cdots + l_N = L} \det[c_{l_1}(\theta_{j_1}), c_{l_2}(\theta_{j_2}), \ldots, c_{l_{N_1}}(\theta_{j_{N_1}})] \\ &\quad \times \det[c_{l_{N_1+1}}(\theta_{j_{N_1+1}}), c_{l_{N_1+2}}(\theta_{j_{N_1+2}}), \ldots, c_{l_N}(\theta_{j_N})] \\ &\quad \times |l_1^{\uparrow}, \ldots, l_{N_1}^{\uparrow}, l_{N_1+1}^{\downarrow}, \ldots, l_N^{\downarrow}\rangle. \end{aligned} \tag{8}$$

The Hamiltonian of a few-electron quantum ring in the perpendicular magnetic fields with parabolic confinement and exact interaction is

$$\begin{aligned} H = &\sum_{i=1}^{N} \left(\frac{(\hat{P}_i + e\vec{A})^2}{2m_e^*} + \frac{1}{2} m_e^* \omega_0^2 (r_i - R_0)^2 \right) \\ &+ \sum_{i<j} \frac{e^2}{4\pi\epsilon |\vec{r}_i - \vec{r}_j|}, \end{aligned} \tag{9}$$

where $\vec{A}$ is the vector potential of the magnetic field and the Zeeman splitting has been ignored. In order to obtain the many-particle states with certain total spin S analytically, we first recourse to a Hamiltonian with simplified form. In the second quantization scheme, the N-localized-electron Hamiltonian can be written formally as

$$H = \sum_i \epsilon_i a_i^{\dagger} a_i + \tfrac{1}{2} \sum_{ijkl} V_{ijkl} a_i^{\dagger} a_j^{\dagger} a_l a_k, \tag{10}$$

where i, j, k, l represent the single-particle orbit functions in equation (1) and $a_i^{\dagger}(a_i)$ is the corresponding creation (annihilation) operator. If the electrons are strictly localized in a single-ring geometry, we can assume a simple interaction form only with formal exchange integrals between neighbor and next-neighbor electrons, which are respectively $V_{i,i\pm1,i\pm1,i} = v_1$ and $V_{i,i\pm2,i\pm2,i} = v_2$. Then the eigenstates of the Hamiltonian of interacting electrons with certain S and S_z can be obtained easily as the linear combinations of the bases in equation (7). Recalling the results of angular momentum projection in equation (8), we will get the states with conserved angular momenta and spins which can be regarded as the many-body trial wavefunctions for spin-dependent RWMs in quantum rings in equation (9).

For example, for the two-electron case with $S_z = 0$, assuming that two localized single-particle orbits are centered at the positions $\theta_j = 0$ and π, respectively, we will have two many-particle bases

$$\begin{pmatrix} |1\rangle \\ |2\rangle \end{pmatrix} = \begin{pmatrix} |Z_1^{\uparrow}, Z_2^{\downarrow}\rangle \\ |Z_2^{\uparrow}, Z_1^{\uparrow}\rangle \end{pmatrix} \tag{11}$$

where Z_1 and Z_2 represent the orbits centered at $\theta_j = 0$ and π, respectively. For the two-electron case, the simplified Hamiltonian with only the interaction between the two orbits is

$$H = \begin{pmatrix} 0 & v_1 \\ v_1 & 0 \end{pmatrix}. \tag{12}$$

The total spin S, energy E and corresponding eigenstates are

$$\begin{aligned} &S = 0, \quad &&E = v_1 \quad &&: \quad (\sqrt{2}/2, \sqrt{2}/2) \\ &S = 1, \quad &&E = -v_1 \quad &&: \quad (\sqrt{2}/2, -\sqrt{2}/2). \end{aligned} \tag{13}$$

According to equation (6) and equation (8), the components of the many-particle bases in equation (11) with angular momentum L are

$$\begin{aligned} |1\rangle_L = &\sum_{l_1 < l_2}^{l_1 + l_2 = L} \left[\prod_{j=1}^{2} \exp\left(-\frac{\lambda^2}{2|R_0|^2} \left(l_j + \frac{\phi}{\phi_0} \right)^2 \right) \right] \\ &\times (-1)^{l_2} |l_1^{\uparrow}, l_2^{\downarrow}\rangle \\ |2\rangle_L = &(-1)^L |1\rangle_L. \end{aligned} \tag{14}$$

Recalling equation (13), it can be found that the two-electron variational trial wavefunctions with angular momentum L is just the component $|1\rangle_L$, and there are selection rules between the angular momenta and the spins of the wavefunctions:

$$\begin{aligned} &S = 0, \quad &&L = 2n \\ &S = 1, \quad &&L = 2n + 1, \end{aligned} \tag{15}$$

where n is an arbitrary integer.

For the three-electron case with $S_z = 0.5$, assuming that the electrons are localized at the vertices of an equilateral triangle, there are three many-particle bases

$$\begin{pmatrix} |1\rangle \\ |2\rangle \\ |3\rangle \end{pmatrix} = \begin{pmatrix} |Z_1^{\uparrow}, Z_2^{\uparrow}, Z_3^{\downarrow}\rangle \\ |Z_1^{\uparrow}, Z_3^{\uparrow}, Z_2^{\downarrow}\rangle \\ |Z_2^{\uparrow}, Z_3^{\uparrow}, Z_1^{\downarrow}\rangle \end{pmatrix}, \tag{16}$$

where Z_1, Z_2 and Z_3 represent three single-particle orbits centered at the vertices of the triangle. Here only the interaction v_1 between the neighboring electrons still needs to be taken into account and the simplified Hamiltonian is

$$H = \begin{pmatrix} -v_1 & v_1 & -v_1 \\ v_1 & -v_1 & v_1 \\ -v_1 & v_1 & -v_1 \end{pmatrix}. \tag{17}$$

The eigenvalues and corresponding eigenstates are

$$\begin{aligned} S=0.5, \quad & E=0 \quad : \quad (\sqrt{2}/2, 0, \sqrt{2}/2) \\ & \qquad\quad\ \ (\sqrt{6}/6, \sqrt{6}/3, \sqrt{6}/6) \\ S=1.5, \quad & E=-3v_1 \quad : \quad (\sqrt{3}/3, -\sqrt{3}/3, \sqrt{3}/3). \end{aligned} \tag{18}$$

Again, using equations (6) and (8), the components of the three-electron many-body bases with total angular momentum L can be obtained and there are still simple relations between them:

$$\begin{aligned} |1\rangle_L = & \sum_{l_1<l_2}^{l_1+l_2+l_3=L} \left[\prod_{j=1}^{3} \exp\left(-\frac{\lambda^2}{2|R_0|^2}\left(l_j+\frac{\phi}{\phi_0}\right)^2\right)\right] \\ & \times \ (\mathrm{e}^{\mathrm{i}\frac{2\pi}{3}l_2} - \mathrm{e}^{\mathrm{i}\frac{2\pi}{3}l_1})\mathrm{e}^{\mathrm{i}\frac{4\pi}{3}l_3}|l_1^{\uparrow}, l_2^{\uparrow}, l_3^{\downarrow}\rangle \end{aligned} \tag{19}$$

$$|2\rangle_L = -\mathrm{e}^{\mathrm{i}\frac{4\pi}{3}L}|1\rangle_L$$

$$|3\rangle_L = \mathrm{e}^{\mathrm{i}\frac{2\pi}{3}L}|1\rangle_L.$$

Then it can be found that the formula of three-electron variational trial wavefunctions with angular momentum L is just the component $|1\rangle_L$, and there are also corresponding selection rules between the angular momenta and the spins of the wavefunctions:

$$\begin{aligned} S=0.5, \quad & L=3n\pm 1 \\ S=1.5, \quad & L=3n, \end{aligned} \tag{20}$$

where n is an arbitrary integer.

For the four-electron case, there are six many-particle bases with $S_z = 0$. According to equations (6) and (8), the explicit form of these bases with total angular momentum L are (up to a constant)

$$\begin{aligned} |k\rangle_L = & \sum_{l_1<l_2, l_3<l_4}^{l_1+l_2+l_3+l_4=L} \left[\prod_{j=1}^{4} \exp\left(-\frac{\lambda^2}{2|R_0|^2}\left(l_j+\frac{\phi}{\phi_0}\right)^2\right)\right] \\ & \times \ \left(\mathrm{i}^{kl_1} - \mathrm{i}^{kl_2}\right)\left(\mathrm{i}^{kl_3} - \mathrm{i}^{kl_4}\right)(-1)^{(l_3+l_4)/k}|l_1^{\uparrow}, l_2^{\uparrow}, l_3^{\downarrow}, l_4^{\downarrow}\rangle \end{aligned} \tag{21}$$

with $k = 1$ and 2, and

$$\begin{aligned} |3\rangle_L &= -\exp(-\mathrm{i}6\pi L/4)|1\rangle_L \\ |4\rangle_L &= -\exp(-\mathrm{i}2\pi L/4)|1\rangle_L \\ |5\rangle_L &= -\exp(-\mathrm{i}2\pi L/4)|2\rangle_L \\ |6\rangle_L &= \exp(-\mathrm{i}4\pi L/4)|1\rangle_L. \end{aligned} \tag{22}$$

According to the similar derivation in two-electron and three-electron cases, it can be found that the four-electron trial wavefunctions with angular momentum L can be expressed as the linear combinations of $|1\rangle_L$ and $|2\rangle_L$ by the consideration of equation (22). We have also done a detailed derivation for four-electron RWMs in quantum dots in previous work [21]; the derivation process here is similar to that. The final four-electron wavefunctions and the angular momentum selection rules for different spin states are

$$\begin{aligned} S=0, \quad & L=4n+2 \quad : \quad |1\rangle_L + |2\rangle_L \\ & L=4n \quad\ : \quad |1\rangle_L \\ S=1, \quad & L=4n\pm 1 \quad : \quad |1\rangle_L \\ & L=4n \quad\ : \quad |2\rangle_L \\ S=2, \quad & L=4n+2 \quad : \quad 2|1\rangle_L - |2\rangle_L. \end{aligned} \tag{23}$$

It should be mentioned that the trial wavefunctions are also suitable for the case without magnetic fields although the above derivations are with full consideration of the field. If $B = 0$, i.e. $l_B \sim \infty$, the phase factor in equation (1) is 1 and it does not alter the following derivations. Of course, B or ϕ in all equations should be taken as zero.

In the following discussions, we will show that the trial wavefunctions in equations (19) and (23) with λ and λ', which minimize the energy, give an accurate description of the electronic states, especially RWMs in quantum rings with appropriate size and shape. Also the selection rules between the spin and total angular momentum of the wavefunction just describe the angular momentum transitions of the lowest states with different spins in magnetic fields.

3. Results and discussions

The values of the variational parameters are determined by minimizing the energy of the wavefunction, so we first present the formula of the energy expectation value of the trial wavefunction. Although we only discuss the scenario without magnetic fields in subsections 3.1 and 3.2, the formula presented here is with full consideration of the fields.

For the quantum rings in equation (9), in order to calculate the energy expectation values of the trial wavefunctions, we can evaluate the kinetic energy $\langle\psi_l|(\hat{P}_i + e\vec{A})^2|\psi_l\rangle$ and confinement energy $\langle\psi_l|(r - R_0)^2|\psi_l\rangle$ of ψ_l in equation (3) at first. Using the definition of $F(k)$ in equation (4), the kinetic energy

$$\begin{aligned} \langle\psi_l|(\hat{P}_i + e\vec{A})^2|\psi_l\rangle = & -\hbar^2\langle\psi_l|\nabla^2|\psi_l\rangle \\ & - \mathrm{i}e\hbar B\langle\psi_l|\frac{\mathrm{d}}{\mathrm{d}\theta}|\psi_l\rangle + \frac{1}{4}e^2B^2\langle\psi_l|r^2|\psi_l\rangle \end{aligned}$$

can be calculated with

$$\begin{aligned} \langle\psi_l|\nabla^2|\psi_l\rangle = & \left[\frac{F(4)}{\lambda'^4} - \frac{2R_0F(3)}{\lambda'^4} + \frac{(R_0^2 - 3\lambda'^2)F(2)}{\lambda'^4}\right. \\ & \left. + \frac{2R_0F(1)}{\lambda'^2} + \left(\frac{1}{4} - l^2\right)F(0)\right] \Big/ F(2) \end{aligned}$$

$$\langle\psi_l|\frac{\mathrm{d}}{\mathrm{d}\theta}|\psi_l\rangle = \mathrm{i}l$$

$$\langle\psi_l|r^2|\psi_l\rangle = F(4)/F(2)$$

and the confinement energy is

$$\langle\psi_l|(r - R_0)^2|\psi_l\rangle = \left(F(4) - 2R_0F(3) + R_0^2F(2)\right)/F(2).$$

Having gotten these expressions, we can calculate the single-particle energy parts of the Hamiltonian equation (9). Then the interaction energy can be evaluated numerically.

3.1. Shape and size effects on RWMs

Having presented the formula of the trial wavefunctions and their energy expectation values, we compare their energies and overlaps with the results of the ED method to demonstrate the applicability of the wavefunctions. In this subsection, we mainly focus on the lowest two electronic states of three-electron and four-electron quantum rings without magnetic

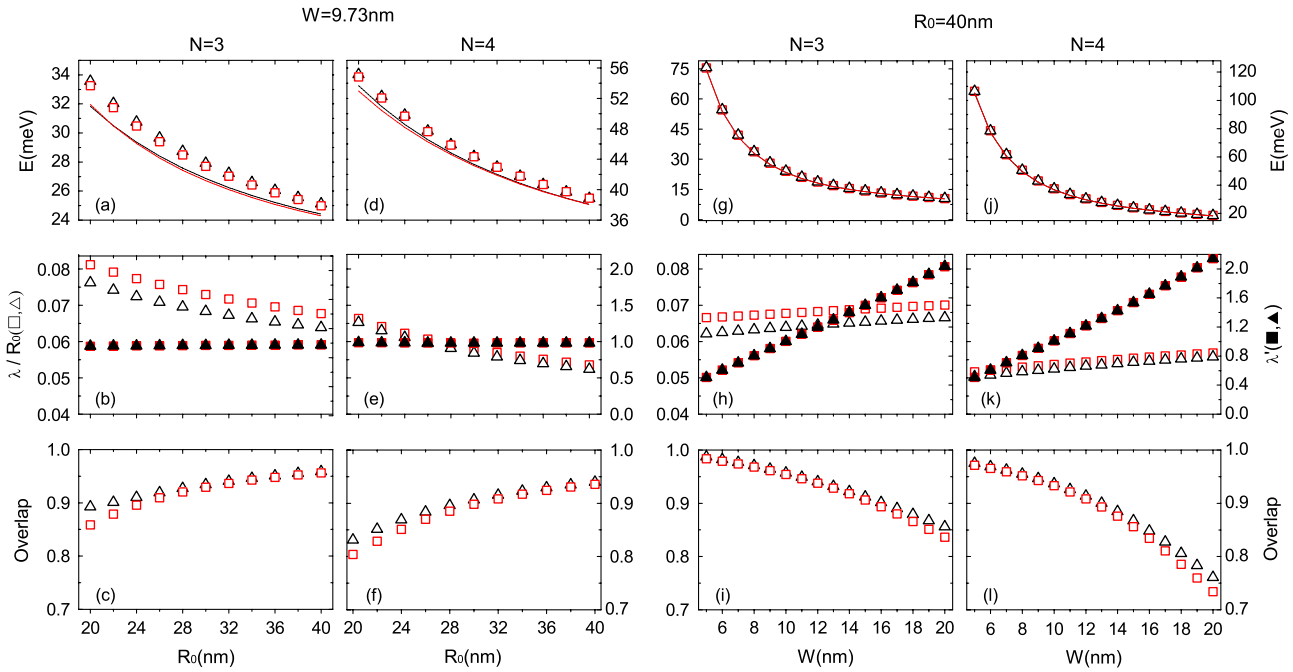

Figure 1. Upper row: the energy expectation values E of the three-electron and four-electron trial wavefunctions as functions of the radius R and width W of the ring. Middle row: corresponding variational parameters λ/R_0 (empty entities) and λ' (filled entities) of the trial wavefunctions. Lower row: overlaps of the trial wavefunctions with the results of the ED method. For the three-electron case, the triangle and square respectively correspond to the states $S = 0.5$, $L = -1$ and $S = 1.5$, $L = 0$. For the four-electron case, they respectively correspond to the states with $S = 0$, $L = 0$ and $S = 1$, $L = 0$. The energies calculated by the ED method are also presented as lines in the upper row.

fields to reveal the meaning of the variational parameters. We will show that the trial wavefunctions with the variational parameters λ and λ' which minimize the expectation value of energy can describe the few-electron RWMs in quantum rings with large radius and small width. The discussions with magnetic fields are left to sections 3.3 and 3.4.

For quantum rings with parabolic confinements, we can define the width of the ring as $W = (2\hbar/m_e^*\omega_0)^{\frac{1}{2}}$. Then the radius R_0 and width W are important structural parameters which may affect the character of the electronic states in quantum rings. So we first compare the energies of the trial wavefunctions and their overlaps with the results of the ED method for the rings with different structure parameters in figure 1, where λ and λ' have been optimized to minimize the energy expectation values. The triangle and square, respectively, represent the three-electron (four-electron) states $S = 0.5$, $L = -1$ ($S = 0$, $L = 0$) and $S = 1.5$, $L = 0$ ($S = 1$, $L = 0$). It can be found that, if the width of the ring is kept unchanged, the trial wavefunctions can give accurate energies and highly overlap with the ED ones for the rings with larger radius. The energy differences between the trial wavefunctions and the ED ones are lower than 1 meV and the overlap can exceed 93% (90%) for the three-electron (four-electron) rings with $W = 9.73$ nm, if $R \geqslant 30$ nm. With the increase of the radius, the accuracy of the trial wavefunctions increases. This is because the degree of the localization in the angular direction increases with the increase of the radius. Then our trial wavefunctions can accurately describe such crystal-like states (RWMs). Also the crystallization greatly depends on the particle number in nanostructures. The smaller the particle number is, the easier the crystallization is. so it can be seen in figure 1 that the accuracy of the three-electron trial wavefunctions is higher than that of the four-electron ones. We have examined the trial wavefunctions in the two-electron case, which also reveals the higher accuracy of the wavefunctions. For example, for the ring with $W = 9.73$ nm and $R \geqslant 30$ nm, the overlap of the trial wavefunctions with the ED ones can be greater than 95%.

With the change of R_0, the variational parameters must also change correspondingly. According to equation (2), it can be anticipated that the value of λ/R_0 must decrease with the increase of R_0 to reflect the increasing localization in the angular direction. This anticipation has been confirmed by our calculation, as shown in figure 1. The plot also shows that the change of λ' with the change of R_0 can be very slight when the radial confinement is unchanged.

Another situation is keeping the radius unchanged and changing the width of the ring. In the third and fourth columns of figure 1 we show the accuracy of the trial wavefunctions with fixed $R = 40$ nm. Here we have chosen a large radius which ensures the localization of electrons in the angular direction. It can be found in the plot that the overlap can be greater than 95%(93%) for the three-electron (four-electron) rings with $W \leqslant 10$ nm. Increasing width means decreasing confinement in the radial direction. According to equation (2), the variational parameter λ' should increase to reflect the delocalization of the electrons in the radial direction, and at this time λ/R_0 only has a slight increase, as shown in figures 1(h) and 1(k). The fact that only one corresponding variational parameter changes when R or W varies just reflects

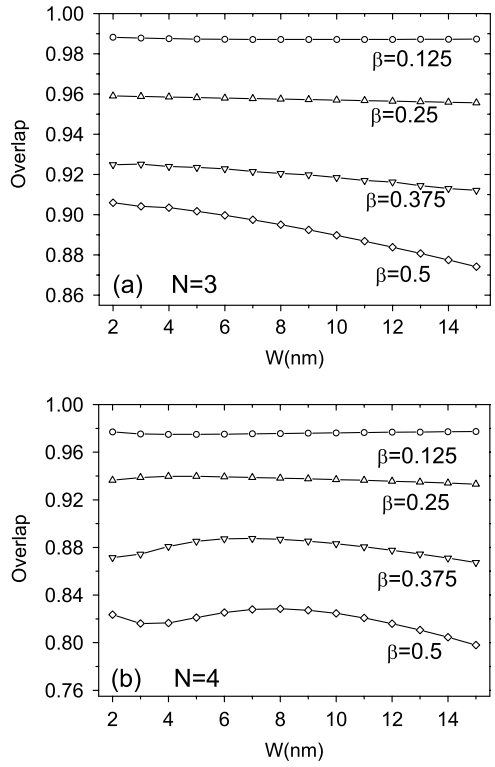

Figure 2. Overlap between the trial wavefunctions and the ED ones with different $\beta = W/R_0$ as a function of the width of the ring for (a) three-electron and (b) four-electron cases. The lines with ○, △, ▽ and ◇ correspond to $\beta = 0.125$, 0.25, 0.375 and 0.5, respectively.

the decoupled nature of the trial wavefunctions in the radial and angular parts.

Figure 1 also shows that the overlaps of the trial wavefunctions with the ED ones decrease with the increase of the width. When the width is quite large, the trial wavefunctions will again obviously deviate from the ED results. The failure of the trial wavefunctions in describing the electronic states in quantum rings with large width is because the radial and angular parts of the real electronic states cannot be decoupled any more.

As a whole, the trial wavefunctions are suitable to describe the crystal-like states in large and narrow rings. Such demand can be quantified by the ratio $\beta = W/R_0$ which describes the shape of the ring. For fixed radius (width), a smaller β corresponds to a narrower width (larger radius), i.e. more ring-like geometry. In figure 2 we can see the effect of the rings' shape on the applicability of the trial wavefunctions. For the rings with smaller β, the trial wavefunctions can highly overlap with the ED results no matter how large the width is. It is because that, for small β, a 'large' width also corresponds to a large radius, which ensures the decoupling of the radial and angular parts of the states, as well as the localization of electrons in the angular direction. With the increase of β, the overlap becomes worse, especially for the rings with larger width. For the three-electron case, the trial wavefunctions can describe the electronic states well for the ring with $\beta \leqslant 0.25$ (the overlap can exceed 95%). For the rings with moderately larger β, as discussed above, the wavefunctions are only applicable to those with smaller width. If $\beta > 0.5$, the nanostructure is actually disc-like; then the wavefunctions are not applicable (the overlap is much lower than 90%). For the four-electron case, the overlap can also be larger than 93% if $\beta \leqslant 0.25$.

In figure 2 there is an interesting fact which should be noticed. For fixed β, smaller width also means smaller radius which may cause delocalization of electrons in the angular direction. Then the real electronic state is the liquid-like one other than the crystal one. As a result, the overlap between the trial wavefunctions and the ED method may decrease. But in figure 2 it can be seen that for the three-electron (four-electron) case, the wavefunctions with $\beta \leqslant 0.5(0.25)$ can still highly overlap with the ED results even if the width is quite small. It should be pointed out that such a fact reflects a character of the trial wavefunctions. In the derivation of the trial wavefunction equations (19) and (21) for RWMs, we have assumed the conditions $\theta \approx \theta_j$ and $R \approx R_0$ to guarantee the equality in the expansion equation (5) when the coefficient c_l is approximated by equation (6). These assumptions can be only satisfied when W and λ/R_0 are small enough. For the rings with small radius, the process of variation with λ which minimizes the energy of the wavefunction may break the assumption since λ/R_0 increases with the decrease of the radius; see the tendency of λ/R_0 in figures 1(b) and (e). Then equations (19) and (21) no longer describe the crystal-like states. However, small β and small W still ensure that the radial and angular parts of the real electronic states are decoupled although the electrons are delocalized in the angular direction. Then such quasi-one-dimensional liquid-like states with decoupled radial and angular parts can also be approximated by wavefunctions with variational parameters describing these two parts, just like equations (19) and (21) do, respectively. This fact makes it possible to discuss the spin rules of the ground state in quantum rings without magnetic fields based on the trial wavefunctions.

3.2. Spin-related orbital occupations

For three-electron quantum rings, previous studies by the ED method have revealed that there is a spin transition of the ground state even without magnetic fields [14]. For fixed β, with the increase of the width W, i.e. the increase of the radius R, the spin of the ground state changes from 0.5 to 1.5, which is accompanied by an angular momentum transition from $L = -1$ to 0. Similar spin transition also exists in the one-dimensional rings with three electrons when increasing the diameter of the ring, but is absent in the four-electron case [16]. Having investigated the accuracy of the trial wavefunctions, we discuss the single-particle orbital occupations in this subsection to understand the spin rules of the three-electron and four-electron ground states with the change of size of the ring.

In figures 3(b) and (c) we show two typical single-particle angular momentum occupations of three-electron trial wavefunctions with different sizes of the ring. With fixed β, decreasing width means decreasing radius. We have seen in figure 1 that λ/R_0 increases with the decrease

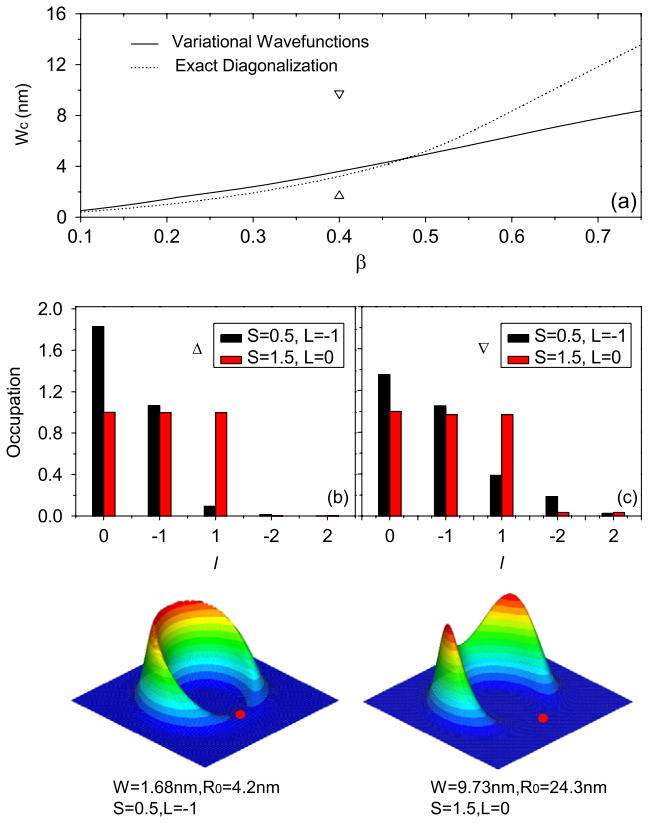

Figure 3. (a) Critical width W_c of three-electron spin transition as a function of β. The solid and dotted lines correspond to the results of trial wavefunctions and the ED method. (b) and (c) The occupations of the single-particle angular momentum components for the states $S = 0.5, L = -1$ and $S = 1.5, L = 0$ with the size of the ring corresponding to the positions marked with $\triangle$ and ∇ in (a). The conditional probability densities of the ground states of the rings with two sizes are also shown in the insets, where the dot indicates the position of the fixed electron.

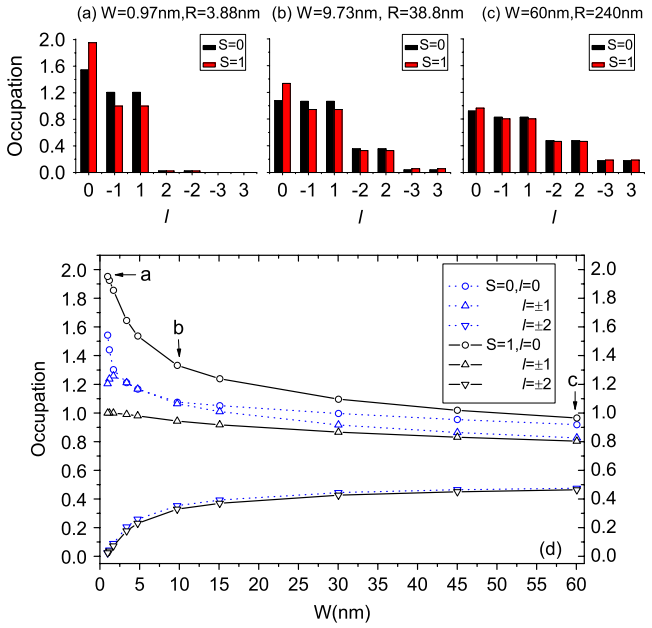

Figure 4. (a)–(c) The single-particle orbital occupations of the four-electron trial wavefunctions with $S = 0$, $L = 0$ and $S = 1$, $L = 0$ with the increase of the width of the ring and fixed $\beta = 0.25$. (d) The change of the occupations of single-particle angular momentum orbits $l = 0, \pm 1$ and ± 2 for the two states as functions of the width of the ring with $\beta = 0.25$. The arrows with a, b and c just indicate the positions corresponding to subfigures (a), (b) and (c).

of R_0. According to equation (6), for the trial wavefunctions with larger λ/R_0, the coefficients of angular momentum components decrease more rapidly with the increase of l. It results in a smaller number of occupied single-particle angular momentum components. When the radius is small enough, for each spin state, only one kind of occupation can survive, see figure 3(b) as an example. It is known that the kinetic energy and the Coulomb interaction are proportional to $1/R^2$ and $1/R$, respectively. For such a small radius, compared with the orbital energy, the interaction between electrons can be almost ignored. Then the spin state with the orbital occupation which has the lowest orbital energy will be the unique ground state. As shown in figure 3(b), for the three-electron case, the state with $S = 0.5, L = -1$ can have two electrons with opposite spins occupy the orbit $l = 0$. So it is the ground state with smaller radius (width). We present the conditional probability density (CPD) of the trial wavefunction $S = 0.5, L = -1$ in figure 3 to explicitly show the particle correlation of the ground state with a small R_0. The CPD is the probability density of finding other electrons in position $\mathbf{r}$ when one electron is fixed. It can be found from the CPD that the trial wavefunction describes a liquid-like state which has no long-range correlation when the radius is small, as discussed in the previous subsection.

With the increase of the width, i.e. the increase of the radius when β is fixed, decreasing λ/R_0 makes the number of occupied orbits increase, as shown in figure 3(c). In such situations, the Coulomb interaction becomes important. Then the spin state with greater average orbital occupation which has lower interaction will become the ground state. For the three-electron case it is just the state $S = 1.5, L = 0$. We also show its CPD in the inset of figure 3, which demonstrates that the trial wavefunction describes the crystal-like state when the radius becomes large.

In figure 3(a), we also plot the critical width W_c as a function of β where the ground state transition from $S = 0.5$ to 1.5 occurs. If the width of the ring is larger than the critical width, the ground state will be the fully polarized state $S = 1.5, L = 0$. The solid and dotted lines correspond to the results of the trial wavefunctions and the ED method, respectively. It can be seen that the two methods give quite similar critical widths when $\beta \leqslant 0.5$, and have an apparent deviation when $\beta > 0.5$. This fact demonstrates again that our trial wavefunctions can describe the electronic states in apparent ring-like geometry.

For the four-electron case with quite small width, i.e. small radius for fixed β, the single-particle orbital occupations of states $S = 1, L = 0$ and $S = 0, L = 0$ are those in figure 4(a). The state with $S = 1$ has lower orbital energy, so it is the unique ground state when the Coulomb interaction can be ignored. In fact, for a further smaller radius than

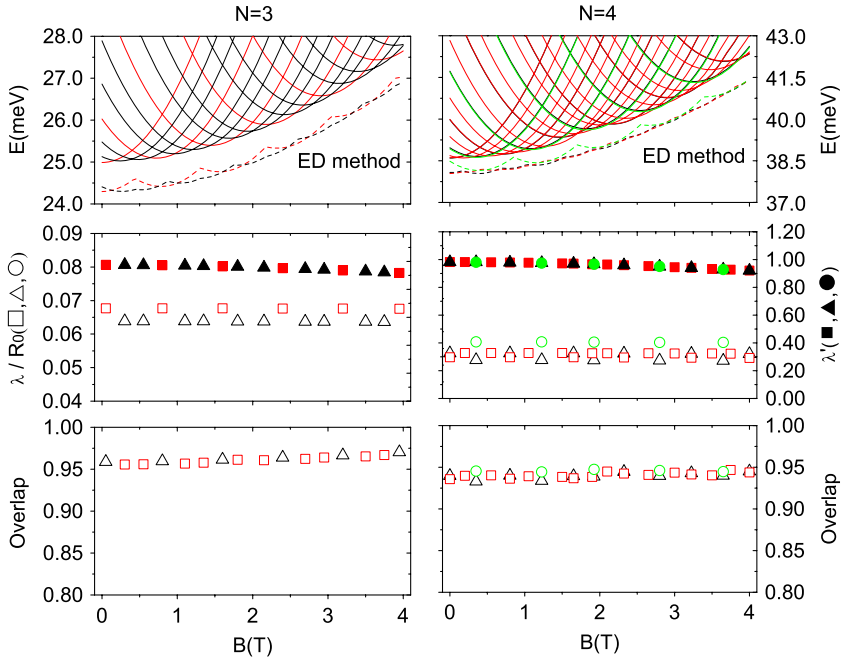

Figure 5. Upper row: energy expectation values E (solid lines) of the trial wavefunctions with different spins for a three-electron (left column) and four-electron (right column) quantum ring with $R = 40$ nm and $W = 9.73$ nm as functions of the magnetic field. The energies of the lowest states calculated by the ED method are also presented as dashed lines. The black, red and green lines correspond to the states with total spin from minimum to maximum. Middle row: corresponding parameters λ/R_0 (empty entities) and λ' (filled entities) of the trial wavefunctions. Lower row: overlaps between the trial wavefunctions and the ED ones. Triangle, square and circle correspond to the states with total spin from minimum to maximum.

that in figure 4(a), the orbital occupations of the two states can tend to be uniform, but the state with $S = 1$ is still the unique ground state because it has lower exchange interaction than the state with $S = 0$. With the increase of the radius, the energy difference of the two states decreases since the Coulomb interaction of the state with $S = 0$ is smaller than that of the state with $S = 1$. When the radius becomes large enough, the orbital occupations of the two states become almost the same, as shown in figure 4(c). In this case, the orbital and the Coulomb energies of the two states become similar. Since the exchange energy becomes very small with quite large radius where the electrons are well localized, the energies of the two states are almost degenerate. So from the analysis of orbital occupation, it can be understood that there is no spin transition for four-electron quantum rings. In figure 4(d), we also present the transitions of the occupation of single-particle angular momentum orbits $l = 0, \pm 1$ and ± 2 for the two states as functions of the width of the ring with $\beta = 0.25$. With the increase of the width, i.e. the increase of the radius of the ring when β is fixed, the correlation between electrons also exhibits the transition from the liquid-like to the crystal-like one, which is similar to the CPDs in figure 3.

The results of the ED method also show that the energies of four-electron states $S = 1, L = 0$ and $S = 0, L = 0$ tend towards being degenerate at large radius, as in the discussion based on the trial wavefunction above. Also the energy difference is typically lower than 0.1% of the total energy. It should be pointed out that the trial wavefunction may give an incorrect energy sequence for such a small energy difference. It is due to a tiny difference between the overlaps of different spin states with the ED ones (for the states $S = 1$ and 0, the overlaps may have a difference which is typically 0.1%–0.5% for $\beta \leqslant 0.25$). In any case, the trial wavefunctions can reveal and give a correct understanding of the tendency of the degeneration of the two states.

3.3. RWMs in magnetic fields

In previous sections, we have investigated the properties of the trial wavefunctions without magnetic fields. We will now discuss the properties of RWMs in magnetic fields based on the trial wavefunctions in this and the next subsections.

For the simplest two-electron case, previous investigation [26] with the ED method has revealed the angular momentum and spin transitions of the ground state $(S, L) : (0, 0) \rightarrow (1, -1) \rightarrow (0, -2) \rightarrow (1, -3)$, etc, which are in accordance with the selection rule in equation (15). So next we examine the three-electron and four-electron cases.

In figure 5, we show the energies of the three-electron and four-electron trial wavefunctions for a quantum ring with $R = 40$ nm and $W = 9.73$ nm with the increase of the magnetic field. The variational parameters λ and λ' have been chosen as the values which minimize the energy of the corresponding state. In the same plot, we also show the energies of the lowest states with different spins calculated by the ED method. Without the Zeeman splitting, there are continuous angular momentum transitions of the ground states and the lowest states with different spins form a narrow band. The angular momenta of the lowest states with different spins obtained from the ED method are still in accordance with the

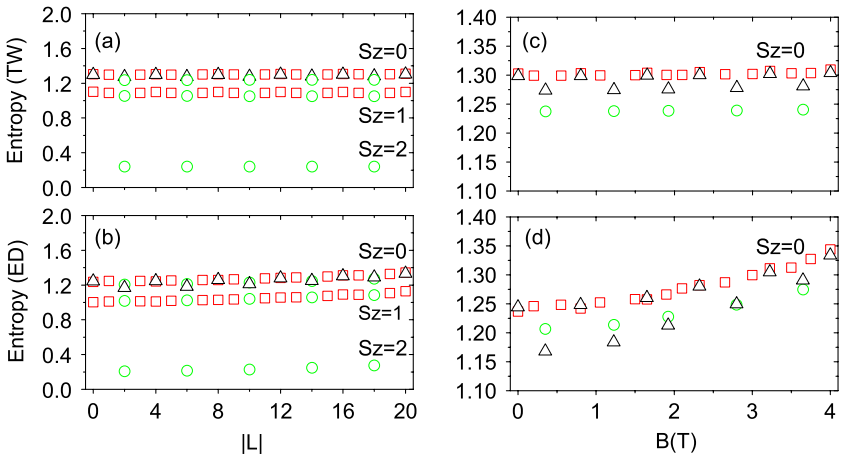

Figure 6. Four-electron entanglement entropy of the lowest states with different S and S_z calculated by (a) the trial wavefunctions and (b) the ED method as functions of the angular momentum. In the plots, the size of the ring is $R = 40$ nm, $W = 9.73$ nm. In order to clearly show the AB oscillations of the entropies, the entropies of the states with $S_z = 0$ as a function of the magnetic field are also shown in (c) and (d). The triangle, square and circle represent the states with $S = 0$, 1 and 2, respectively.

rules in equations (20) and (23). The energy level sequences of the lowest states of the trial wavefunctions are the same as the ED ones. It means that the trial wavefunctions can correctly describe the angular momentum transitions of different spin states in magnetic fields.

It can be found in figure 5 that the deviations of the energy expectation values of the trial wavefunctions from the ED results are quite small. The energy differences of the two methods within the whole range of the field are no more than 1 meV. The overlaps of the trial wavefunctions with the ED results can be greater than 95%(93%) for the three-electron (four-electron) case. With the increase of the field, the degree of crystallization of electrons increases. Then the overlap between our trial wavefunctions and the ED ones will also increase. In figure 5, the confinement caused by the magnetic field is weaker than the ring's parabolic confinement, so the increase of the overlap is not very notable. Similarly, the changes of the variational parameters are also very slight. For the rings with larger width, the increasing magnetic field will improve the accuracy of the wavefunctions greatly.

It is known that for quantum rings in a strong interaction regime, the energy scale of spin dynamics is much smaller than that of the orbital motion, which indicate the spin–charge separation in the system. Also the spin excitations can be described by a exchange–interaction term [12]. In figure 5 and the above discussion, we have seen that the trial wavefunctions can give the correct energy level sequence and accurately describe the lowest states with different spins in the whole range of magnetic fields. And, with the increase of the magnetic field, along with the angular momentum transitions, the alternations of energy level sequence just reflect the spin excitations in quantum rings. So it means that the trial wavefunctions with different spins describe the low-lying spin excitations in large and narrow quantum rings. This can be attributed to the fact that the simplified formal Hamiltonian, which we adopt to obtain the eigenstates of S, just contains the exchange interaction between localized orbits, see equations (12) and (17).

Before ending this section, it is worthwhile to present a brief discussion of the character of spin correlations of RWMs. For quantum dots, both the ED method and the analytical theories have pointed out that the four-electron crystal states with different spins have specific spin correlations with respect to the angular momentum [2, 22, 29]. For quantum rings, if the localized electrons form a single-ring geometry, our trial wavefunctions can explicitly show the spin correlation rules, since the components $|1\rangle_L$ and $|2\rangle_L$ respectively exhibit the ferromagnetic and anti-ferromagnetic correlations between electrons. And it can be found that the spin correlation rules are just the same as that in quantum dots. This is because these spin correlations originate from the rotational symmetry of RWMs and the ring-like confinement will not affect them. It is also known that the electrons may form multi-ring geometries in quantum dots if there are more than five electrons. The character of spin correlations in those complicated cases is still an open problem. However, it can be anticipated that the confinement of quantum rings will greatly affect the formation of RWMs with multi-ring geometries and, of course, the corresponding spin correlations.

3.4. Entanglement in quantum rings

The RWMs are states with strong quantum correlations, so we next investigate the entanglement, i.e. quantum correlation given by the trial wavefunctions. For an identical-particle state, it is not convinced how to quantify all the entanglement properties, but it is indeed demonstrated that the von Neumann entropy [27, 28] can quantify the entanglement between one electron and the other parts of the system. Having got a many-body wavefunction, the entropy can be calculated by $S = -\mathrm{Tr}[\rho \ln \rho]$, where $\rho_{\mu,\nu} = \langle\psi|a_\mu^+ a_\nu|\psi\rangle$ is the reduced single-particle density matrix [28]. For identical-particle states, ρ does not depend on the choice of the electron.

As discussed above, with the change of the magnetic field, there are angular momentum transitions of the lowest states with different spins in quantum rings. In figure 6, we show

the entanglement entropies of these lowest states for a four-electron quantum ring as functions of the angular momentum. In the plots, not only the results with $S_z = 0$ but also those with $S_z = 1$ and 2 are presented. It can be seen that both the trial wavefunction and the ED method show the S_z dependence of the entropies. The entropies of the states with different S_z but same S are only approximately different by a certain constant. In particular, the values for the states with the smallest and largest S_z are just different by one, as shown in the plots. This is a character of the spin-dependent RWMs, which also exists in quantum dots [21].

According to equation (21), it can be found that, if λ/R_0 is unchanged, the occupied single-particle angular momentum orbits in the trial wavefunctions with total angular momentum L and $L \pm N$ can only be different by a translation $l_j \sim l_j \pm 1$ when the magnetic flux is changed by $\mp\phi_0$. Such states will have the same entanglement entropy, since their reduced single-particle density matrices have the same eigenvalues, and then the same trace. In the previous discussion we have shown that, in the angular momentum transitions of the lowest states with different spins, the change of λ is quite small when the field is not very strong. So there will be Aharonov–Bohm (AB) oscillation of the entropy in the results of the trial wavefunctions since the states with angular momenta L and $L \pm N$ can have almost the same entropy. Figure 6(a) has shown such a conclusion. In figures 6(c) and (d), we show the entropy oscillations of the lowest states with $S_z = 0$ with respect to the field other than angular momenta for clarity. In figure 6(c), the AB oscillations of entropies of different spin states calculated by the trial wavefunctions are clear, and there is a tiny increasing tendency for all spin states. In figure 6(d), it can be found that the results of the ED method also show AB oscillations of entanglement entropies. However, with the increase of the field, the increasing tendency of entropies given by the ED method is more apparent due to the increasing crystallization. And, with the increase of the field, the difference between the results of the ED method and the trial wavefunctions gradually decreases.

It is worthwhile pointing out that the AB oscillation of entropies can also be expected even if there is only an enclosed magnetic flux, but no magnetic field on the ring. For the rings with large radius and small width, the center of mass and relative angular motion can be decoupled. Previous studies have demonstrated that the change of the magnetic flux leads to the angular momentum (rotation of the center-of-mass) transitions of the lowest states with different spins, but does not affect the relative-motion parts of the states [30, 31]. Because the entropy of a state is only decided by its relative-motion part, there will be entropy oscillations in the angular momentum transition with the change of flux.

In figure 7, we take the four-electron states with $L = 0$, $S = 0$ and $S = 1$ as examples to show the size dependence of the entanglement entropies in quantum rings. The sizes have been restricted in the range where the electronic states are crystal-like ones. In figure 7(a), it can be seen from both the results of the trial wavefunctions and the ED method that the entropies increase if the radius of the ring increases. It reflects the fact that the quantum correlation increases when

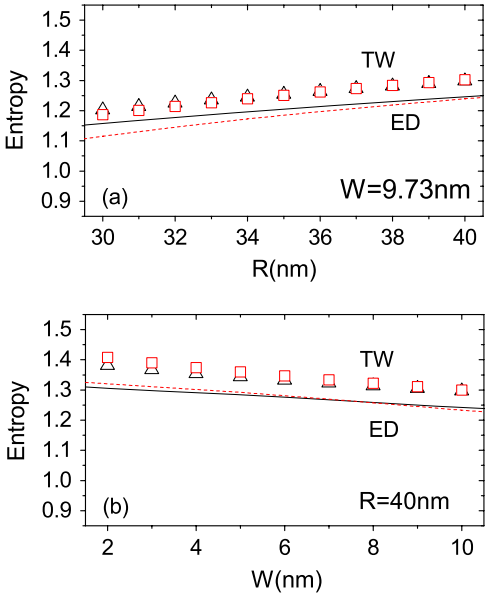

Figure 7. Entanglement entropies of the state $S = 0$, $L = 0$ and $S = 1$, $L = 0$ with $S_z = 0$ calculated by the trial wavefunctions (triangle and square) and the ED method (solid and dotted lines) as functions of (a) the radius R of the ring with $W = 9.73$ nm and (b) the width W with $R = 40$ nm.

the degree of crystallization enhances. The scenario is similar when the width of the ring decreases, see figure 7(b). In fact, for RWMs, both increasing the radius with fixed width or decreasing the width with fixed radius makes λ/R_0 decrease. It broadens the single-particle angular momentum occupation and makes the entropy increase. The entropies given by the trial wavefunctions are higher than those given by the ED method, which means that the trial wavefunctions generally exhibit a higher degree of particle localization than the ED ones.

4. Summary

To conclude, the trial wavefunctions for spin-dependent rotating Wigner molecules in few-electron quantum rings with different shapes and sizes can be constructed from a set of single-particle orbits with two variational parameters. The projection operator technique is employed to restore the rotational symmetry of the wavefunctions. The shape and size-dependent variational parameters can correctly describe the localization of orbits in strong ring-like confinement and ensure that the functions give accurate energies and highly overlap with the results of the exact diagonalization method, no matter whether the magnetic field is present or not.

With the change of the ring shape and size, the trial wavefunctions reveal the transitions of the single-particle angular momentum components of the low-lying states, which are reflected in the transition of particle correlation and can give an understanding of the spin and angular momentum rules of the ground states without the magnetic fields. In magnetic fields, the trial wavefunctions correctly show the angular momentum transitions of the lowest states with different spins.

The AB oscillation of the entanglement entropy of RWMs in quantum rings can be understood by inspecting the nature of the trial wavefunctions with the change of the magnetic flux. The wavefunctions also reveal the spin and size dependence of entropy correctly. With the increase of the magnetic field, the radius or the confinement of the ring, the entanglement entropies increase. Such trial wavefunctions can be used in the studies of quantum behaviors of RWMs in quantum rings and will be helpful in the understanding of few-body physics in nanostructures.

Acknowledgments

Financial support from the NSF China (grant nos. 10574077 and 10774085), the '863' Program of China (no. 2006AA03Z0404) and the MOST Program of China (no. 2006CB0L0601) is gratefully acknowledged.

References

[1] Reimann S M and Manninen M 2002 *Rev. Mod. Phys.* **74** 1283
[2] Koskinen M, Reimann S M, Nikkarila J P and Manninen M 2007 *J. Phys.: Condens. Matter* **19** 076211
[3] Szafran B, Peeters F M, Bednarek S, Chwiej T and Adamowski J 2004 *Phys. Rev.* B **70** 035401
[4] Yannouleas C and Landman U 2002 *Phys. Rev.* B **66** 115315
[5] Yannouleas C and Landman U 2003 *Phys. Rev.* B **68** 035326
[6] Yannouleas C and Landman U 2004 *Phys. Rev.* B **70** 235319
[7] Lorke A, Luyken R J, Govorov A O, Kotthaus J P, Garcia J M and Petroff P M 2000 *Phys. Rev. Lett.* **84** 2223
[8] Viefersa S, Koskinen P, Deo P S and Manninen M 2004 *Physica* E **21** 1
[9] Fuhrer A, Luscher S, Ihn T, Heinzel T, Ensslin K, Wegscheider W and Bichler M 2001 *Nature* **413** 822
[10] Bayer M, Korkusinski M, Hawrylak P, Gutbrod T, Michel M and Forchel A 2003 *Phys. Rev. Lett.* **90** 186801
[11] Voit J 1995 *Rep. Prog. Phys.* **58** 977
[12] Koskinen M, Manninen M, Mottelson B and Reimann S M 2001 *Phys. Rev.* B **63** 205323
[13] Hu H, Zhu J-L and Xiong J-J 2000 *Phys. Rev.* B **62** 16777
[14] Zhu J-L, Hu S, Dai Z S and Hu X 2005 *Phys. Rev.* B **72** 075411
[15] Liu Y M, Bao C G and Shi T Y 2006 *Phys. Rev.* B **73** 113313
[16] Saiga Y, Hirashima D S and Usukura J 2007 *Phys. Rev.* B **75** 045343
[17] Maksym P A 1996 *Phys. Rev.* B **53** 10871
[18] Maksym P A, Imamura H, Mallon G P and Aoki H 2000 *J. Phys.: Condens. Matter* **12** R299
[19] Li Y, Yannouleas C and Landman U 2006 *Phys. Rev.* B **73** 075301
[20] Yannouleas C and Landman U 2002 *J. Phys.: Condens. Matter* **14** L591
[21] Dai Z S, Zhu J-L, Yang N and Wang Y Q 2007 *Phys. Rev.* B **76** 085308
[22] Shi C, Jeon G S and Jain J K 2007 *Phys. Rev.* B **75** 165302
[23] Jeon G S, Chang C C and Jain J K 2004 *J. Phys.: Condens. Matter* **16** L271
[24] Jeon G S, Chang C C and Jain J K 2004 *Phys. Rev.* B **69** 241304(R)
[25] Yannouleas C and Landman U 2007 *Rep. Prog. Phys.* **70** 2067
[26] Hu H, Zhu J-L and Xiong J-J 2000 *Phys. Rev.* B **62** 16777
[27] Paškauskas R and You L 2001 *Phys. Rev.* A **64** 042310
[28] Zeng B, Zhai H and Xu Z 2002 *Phys. Rev.* A **66** 042324
[29] Reimann S M, Koskinen M, Yu Y and Manninen M 2006 *New J. Phys.* **8** 59
[30] Wendler L, Fomin V M, Chaplik A V and Govorov A O 1996 *Phys. Rev.* B **54** 4794
[31] Zhu J-L, Dai Z S and Hu X 2003 *Phys. Rev.* B **68** 045324